Preliminary investigation of the inhibitory effects of mechanical stress in tumor growth

Ishita Garg, Michael I. Miga

Department of Biomedical Engineering, Vanderbilt University, 2201 West End Ave., Nashville, TN 37235

ABSTRACT

In the past years different models have been formulated to explain the growth of gliomas in the brain. The most accepted model is based on a reaction-diffusion equation that describes the growth of the tumor as two separate components- a proliferative component and an invasive component. While many improvements have been made to this basic model, the work exploring the factors that naturally inhibit growth is insufficient. It is known that stress fields affect the growth of normal tissue. Due to the rigid skull surrounding the brain, mechanical stress might be an important factor in inhibiting the growth of gliomas. A realistic model of glioma growth would have to take that inhibitory effect into account. In this work a mathematical model based on the reaction-diffusion equation was used to describe tumor growth, and the affect of mechanical stresses caused by the mass effect of tumor cells was studied. An initial tumor cell concentration with a Gaussian distribution was assumed and tumor growth was simulated for two cases- one where growth was solely governed by the reaction-diffusion equation and second where mechanical stress inhibits growth by affecting the diffusivity. All the simulations were performed using the finite difference method. The results of simulations show that the proposed mechanism of inhibition could have a significant affect on tumor growth predictions. This could have implications for varied applications in the imaging field that use growth models, such as registration and model updated surgery.

Keywords: modeling, disease characterization, image-guided therapy, neurosurgical procedures, registration

1. INTRODUCTION

There are an estimated 13,000 deaths and 18,000 new cases every year for all primary malignant brain and central nervous system (CNS) tumors. This translates to an age-adjusted incidence rate of about 9 per 100,000 people. Gliomas, primary tumors of the supporting tissue of the nervous system, account for 77% of all primary malignant brain tumors [1]. Histologically gliomas are classified as astrocytomas or oligodendrogliomas and pathologically they are subclassified by grades depending on the proliferative potency of the tumor. Clinically the most common presentation of glioma are seizures, headache, mental change and hemiparesis [2]. The differential diagnosis of brain neoplasm is made based on history and exam. The confirmation of diagnosis is typically obtained by some imaging modality, gadolinium enhanced magnetic resonance imaging (MRI) being the current standard. The prognosis depends on the age of the patient at diagnosis and the histologic tumor type. In a 2005 report the Central Brain Tumor Registry of the United States (CBTRUS) reported that glioblastoma (the highest grade glioma) accounted for ~62% of the 20,974 cases of glioma in a period from 1998 to 2002 [3]. In general less than 30% of patients under 45 survive for more than 2 years. For patients over 65 that survival rate dips to an even bleaker ~2% [1]. In the recent past, research efforts to combat this deadly disease have been tremendous in fields ranging from epidemiology, biomedical engineering, genetics to molecular biology. Epidemiology studies study the patterns of glioma prevalence in the society to devise better screening. The engineering aspect is focused on new chemotherapy agents and surgical advances such as intraoperative image guidance. Basic sciences aim to answer fundamental questions about the mechanism of glioma initiation and growth, which could contribute to better screening as well as therapy. Animal models and in vitro techniques have been indispensable for all this research and have aided the testing of mechanistic hypothesis and potential of chemo-therapeutic agents.

Mathematical modeling can also be a valuable tool to understand various factors that initiate, promote, and inhibit tumor growth. Tumor growth has been historically described by an exponential model, a Gompertz model or a logistic model. The aggressive invasion of healthy tissue makes gliomas unique. Glioma growth has been mathematically described in literature by a reaction-diffusion model [4], [5]. This model describes the rate of change of

tumor cell concentration as a contribution of two components: proliferation and invasion. The proliferative component is typically described by a constant growth rate, leading to exponential growth. The invasive component is described by passive Fickian diffusion. Gliomas are known to invade white matter more aggressively than grey matter and Swanson et. al. accounted for this heterogeneous behavior by assigning a higher diffusion coefficient to white matter than gray matter (factor of 2-100) [4]. Several studies extending the reaction-diffusion model have since been published. Jbabdi et. al. used diffusion tensor imaging (DTI) for increased accuracy of anisotropic diffusivity [6]. Clatz et. al., in addition to using anisotropy information from DTI, also coupled the diffusion to mechanics and studied the deformation caused by glioma growth [7].

In vitro techniques when combined with mathematical models can become even more powerful tools for analysis. Stein et. al. successfully combined these techniques and provided quantitative comparisons between theory and experiment for glioblastoma growth mechanism [8]. In a landmark experimental paper Helminger et. al. demonstrated that multicelluar tumor spheroids cultivated in mechanically resistant matrix grow until a threshold level of stress is attained [9]. Several studies describing mathematical models for the results presented in the paper have been published since [10], [11]. These studies use a system of coupled equations describing tumor cell concentration, nutrient concentration, and mechanical stress to model the phenomenon seen in vitro. Ambrosi et. al. use a non-linear elastic model [10] and Roose et. al. used a linear poroelasticity model [11]. In each case, the stress modulates tumor concentration via a coupling relationship.

There is a dichotomy in the literature of mathematical modeling of gliomas between models formulated for in vitro multicellular tumor spheroids and in vivo animal or human tumors. The mathematical models for latter tend to be more simplistic with fewer parameters such as the reaction-diffusion model with a proliferation constant and a diffusion constant. The models for explaining in vitro growth tend to be more complex and have a lot more parameters. Those parameters might be evaluated more easily for the in vitro models, however the increase in number of unknown parameters for macroscopic tumors in human subjects decreases simulation tractability. Ultimately in vitro tumor models provide understanding of basic growth and inhibitory mechanisms which, under careful consideration of those effects, can then be applied to macroscopic scales. Whereas multicellular tumor spheroids grow to a size of several micrometers, in vivo tumors (and gliomas) have a minimum threshold radius of a few millimeters for detection in common imaging modalities. Whereas every finding in vitro tumors may not be directly applicable to tumors some of the findings deserve to be examined in that light. The inhibitory effect of stress for glioma growth might be a significant factor since it grows in the confined space of the cranium. The goal of this paper is to attempt to bridge the gap between these two areas by formulating a simplistic mathematical model for macroscopic glioma growth that accounts for the inhibitory effect of mechanical stress. In the following sections the mathematical model will be introduced, its implementation will be discussed, and the results of simulation experiments using the model will be presented.

2. METHODS

2.1 Mathematical Model

The evolution of tumor cell concentration, c, is modeled by a reaction-diffusion equation similar to [4] as shown below,

$$\frac{\partial c}{\partial t} = \nabla \cdot (D\nabla c) + f(c) \qquad (1)$$

where D is the diffusion coefficient. The first term on the right hand side is the invasive component and represents the spreading of tumor driven by the concentration gradient. The second term represents the proliferative component represented as some function of the cell concentration. In our simulations, the proliferation is modeled by a logistic growth law, i.e.

$$f(c) = \beta(1 - \alpha c)c \qquad (2)$$

α and β are proliferation components in logistic growth. This represents an initial exponential growth which slows down eventually as the nutrients are consumed. This is physiologically consistent as brain parenchyma has a maximum carrying capacity for tumor cells, which has been shown to be around 3.5×10^4 cells/mm^3 [12].

The mechanical equilibrium equation describing the stresses in the system is shown below,

$$\nabla \cdot \sigma + f_{ext} = 0 \qquad (3).$$

Here σ is the stress tensor and f_{ext} is the sum of external forces acting on the system. The material was modeled as a linear elastic system. Details about the constitutive equations can be found in the appendix.

The inhibitory effect on growth by stress was implemented by coupling the diffusion coefficient to stress by an exponential decay relationship shown here,

$$D' = De^{-k\bar{\sigma}} \qquad \qquad (4),$$

where D' is the spatially varying diffusion coefficient and D is invariant diffusion constant, k is a scaling constant and in the above equation $\bar{\sigma}$ represents a yield stress such as Von Mises stress in this case. It is being hypothesized that the mechanical stress inhibits glioma growth by affecting its diffusion coefficient. Gliomas are characterized by an aggressive invasion of parenchyma and a decrease in diffusivity of tumor cells would physiologically produce the observable effect of increase in cell density over time. To this effect an exponential decay relationship was used between the yield stress and diffusion coefficient and the choice was made because of simplicity.

2.2 Implementation

Three different implementations of the basic model presented above were devised. An initial concentration with a normal distribution was used and equation (1) was solved with Neumann boundary conditions of zero flux. In the first implementation, there was no coupling between the diffusion coefficient and stress i.e. cell concentration depended on the reaction-diffusion equation (equation (1)) only. This implementation will be referred to as 'Model 1'. In the other two implementations the diffusion coefficients were coupled to stress by equation (4), but the way the mechanical equilibrium equations were implemented differ. In the second implementation cell concentration gradients contribute to the external forces, i.e.

$$f_{ext} = \lambda \nabla c \qquad \qquad (5).$$

Here λ is a scaling constant. Dirichlet condition of zero displacement was used at outer boundary because tumor cannot diffuse across the skull. Stress free conditions were used on the inner boundary. This model will be referred to as 'Model 2'. This model is similar to approach proposed in [7] to calculate stresses. In the third implementation the mechanical equilibrium was driven by displacements of the tumor front. It was assumed that the mechanical stress does not start to inhibit tumor growth until a certain threshold size is reached. Equation (3) is solved with Dirichlet conditions at both the inner and outer boundaries. At the inner boundary the displacement is given by the difference in the position of the tumor front at that time step and the threshold size. At the outer boundary zero displacement is used as in 'Model 2'. This implementation of the model will be referred to as 'Model 3'. It's worthwhile to note here that the mechanical domain in 'Model 3' only consists of the portion of the tumor cell domain that excludes the threshold tumor size. In the following simulations, the results of these three models will be compared to each other.

2.3 Simulation Experiments

All the implementations were simulated using the finite difference approach in MATLAB. The time dependant equation (1) was solved with an explicit Euler scheme. The parameter values used for the simulations are tabulated in Table 1.

Table 1: Parameter values used for model simulations

Parameter	Symbol	Value
Diffusion coefficient	D	0.001 cm^2/day
Logistic growth parameter	α	1 day^{-1}
Logistic growth parameter	β	0.05 day^{-1}
Young's modulus	E	2100 Pa
Poisson's ratio	υ	0.45

Some of these values were drawn from literature and others were determined by numerical experimentation. For instance the value of diffusion coefficient is quite similar to the value used in [5]. A higher proliferation rate than [5] was used in this case because the value used in that paper caused a sharp drop in cell concentration in the beginning due to high diffusion and low proliferation rate. The mechanical properties of brain tissue i.e. the Young's modulus and Poisson's ratio were found in [13].

3. RESULTS

The tumor cell concentration profiles obtained with the reaction-diffusion model using the logistic growth term are shown in Figure 1.
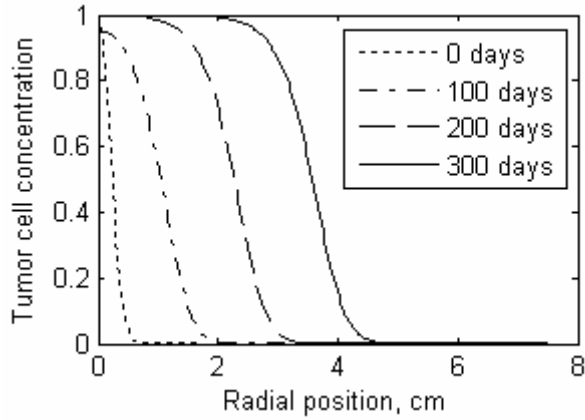
Figure 1: Traveling wave solutions for the reaction-diffusion equation (equation(1)) for tumor cell concentration. The concentration is normalized between a value of 0 and 1. The concentration distribution at 4 different time points is shown.

The figure shows tumor cell concentration profiles at four different time points. The cell concentrations in the figure are scaled between values of 0 and 1. The logistic growth caps the concentration at a certain maximum value. This approach, in our opinion, has a slight advantage over an implementation such as [7] where the exponential growth term is used and the cell concentration is manually constrained in the software beyond a certain maximum value. The concentration profiles follow travelling wave type solutions. It is worth pointing out that the peak concentration falls initially (100 days) while there's a greater spatial spread of the tumor. As the model progresses in time, the peak value is regained. This could be because of the choice of parameters. Initially the diffusion is dominant which spreads the tumor cells across the domain. Then as proliferation catches up, the peak concentration rises again while the tumor cells continue to invade healthy parenchyma.

The tumor cell concentration profiles obtained by the three models at different time points are shown in Figure 2.
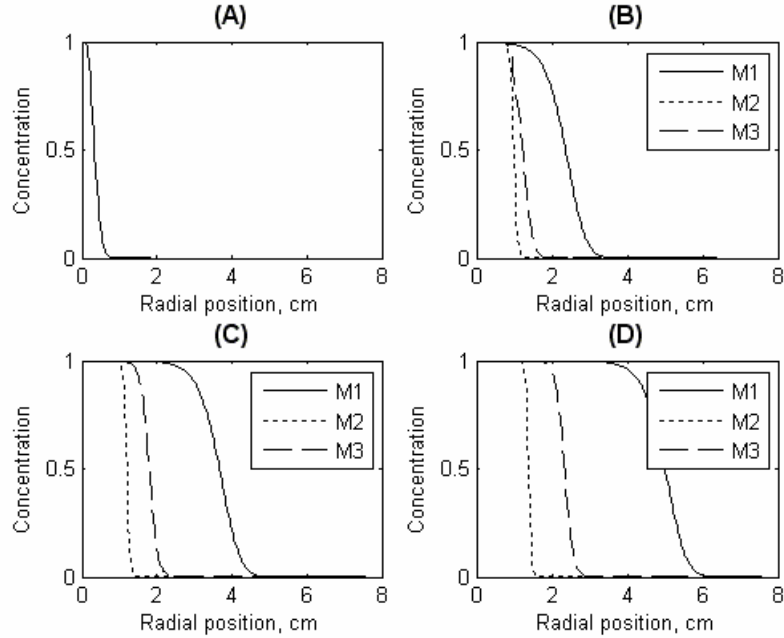
Figure 2: Comparison of the concentration profiles over time for three models. M1 refers to Model 2, M2 to Model 2 and M3 to Model 3. (A) shows the initial cell concentration and (B-D) shows the cell concentrations predicted by the models at 200, 300, and 400 days respectively.

The panel (A) shows the initial tumor cell concentration, which was common to all three models. Panels (B) through (D) show the tumor cell concentrations at 200, 300, and 400 days respectively as predicted by the three models. In each case Model 1, the simple reaction-diffusion model predicts the highest invasiveness for the tumor, followed by Model 3 and Model 2. At 200 days the concentration profiles predicted by Model 2 and Model 3 are relatively similar, but they diverge at future time points. The inhibitory effect in Model 2 is the greatest in part because in Model 3 it is assumed that the tumor grows freely without any effect of mechanical inhibition until it reaches a certain threshold size. In Model 2 stresses exert an inhibitory effect on growth from the beginning of model propagation. However, even when accounting for a quicker start, the rate of invasion is slower for Model 2. The stresses and thus the diffusion coefficients are dependant on the choice of 'k' in equation (4) and λ in equation (5) in Model 2. In Model 3, the diffusion coefficients are dependent only on 'k'. 'k' was kept consistent between the simulations for Model 2 and Model 3. As in [7], λ was an empirically determined parameter and it's choice would explain the discrepancy in observed tumor profiles for Model 2 and Model 3.

The resulting radial displacements, radial stresses, and angular stresses for the three models are shown in Figure 3, Figure 4, and Figure 5 respectively.
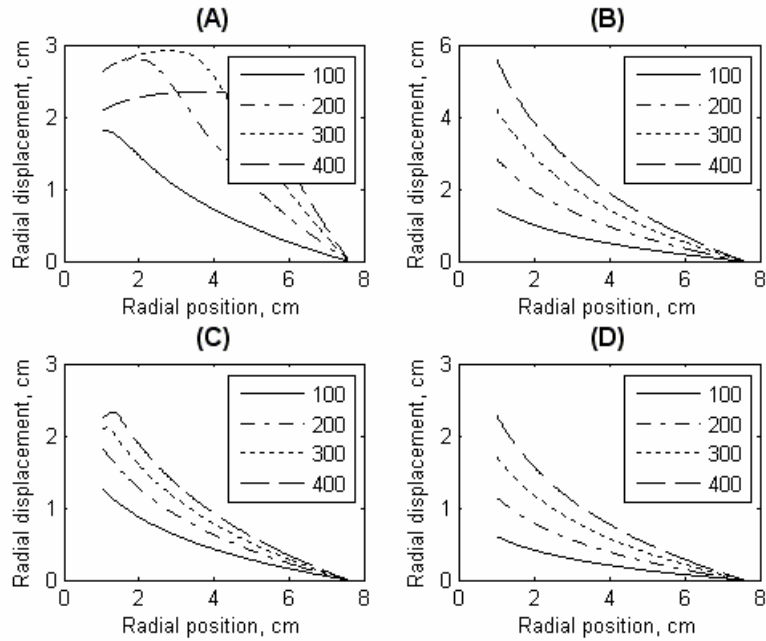
Figure 3: (A) and (B) show the brain tissue displacement in the radial direction for Model 1. In (A) the displacement was calculated by driving the mechanical equilibrium equation by the tumor cell concentration gradient and in (B) they were calculated by driving the mechanical equilibrium equation by the tumor front displacement. (C) and (D) show the results of radial displacements calculated by Model 2 and Model 3.
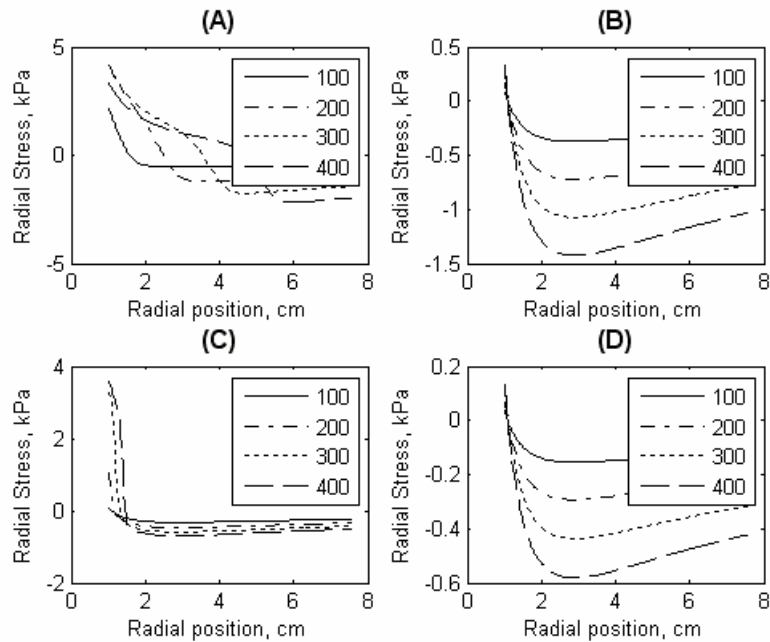
Figure 4: (A) and (B) show the radial stress in the brain tissue for Model 1. In (A) the radial stress was calculated by driving the mechanical equilibrium equation by the tumor cell concentration gradient and in (B) it was calculated by driving the mechanical equilibrium equation by the tumor front displacement. (C) and (D) show the results of radial stess calculated by Model 2 and Model 3.
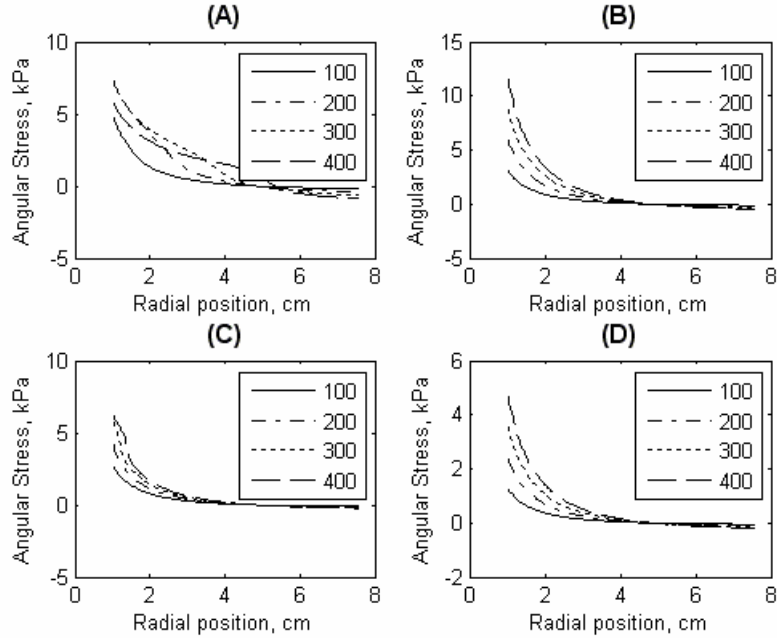
Figure 5: (A) and (B) show the angular stress in the brain tissue for Model 1. In (A) the angular stress was calculated by driving the mechanical equilibrium equation by the tumor cell concentration gradient and in (B) it was calculated by driving the mechanical equilibrium equation by the tumor front displacement. (C) and (D) show the results of angular stress calculated by Model 2 and Model 3.

In each case panels (A) and (B) show the results predicted by Model 1. Results for panel (A) were computed by driving the mechanical equilibrium equation with tumor cell concentration gradients (similar to Model 2). In panel (B) the results were computed by driving the mechanical equilibrium equation by tumor front displacements (similar to Model 3). Panels (C) and (D) show the results obtained from Model 2 and Model 3 respectively. As clarification, the difference between the first two panels and the last two panels is that for each case in (A) and (B) diffusion coefficients were not coupled to stress. The values predicted by all three models are on the same order of magnitude. Comparing the first two panels to the last two, the magnitudes of all three quantities are highest for Model 1. When comparing the displacements in Figure 3 (A) to Figure 3 (B) the displacements predicted by Model 1 are greater than Model 2 at 100, 200, and 300 days. The dip in the displacements at 400 days for Model 1 (Figure 3 (A)) is unexpected since all other curves indicate an increase in displacement values as the model progresses in time. However, the results viewed in confluence with cell concentration gradients at the respective time points explain the dip. Initially there are larger concentration gradients in the inner portion of the domain and towards the exterior the gradient is very small. As the model progresses in time the cell concentration in the interior part of the domain level off due to logistic growth. Thus the cell concentration gradient is lowest close to the inner and outer boundary and highest in between. These gradients acting as an external force to drive mechanical equilibrium explain the observed results. The peaks in radial displacement curves in Figure 3 (A) and (B) correspond to the position of the highest cell concentration gradient at that time point. Radial displacements in Figure 3 (C) and (D) obtained from Model 1 and Model 3 respectively show consistently increasing displacements as model propagates in time, with lower displacement at each time point for Model 3. The radial stresses (Figure 4) are compressive in most of the domain which is expected since tumor growth would create a mass effect, pushing the healthy tissue closer to rigid skull boundary. Closer to the inner boundary the stresses are tensile. The tensile component is much stronger in Model 2 than Model 3. The value of compressive component of stress is quite similar in magnitude for all models. The angular stresses (Figure 5) in all cases are tensile. This trend is also expected since healthy brain parenchyma is modeled as a nearly incompressible material (Poisson's ratio of 0.45). Thus if the tissue is being compressed radially, it would experience stretching in the angular direction.

4. DISCUSSION

The goal of this work was to asses the applicability of knowledge gained from in vitro tumor growth models to human glioma growth. In the past in vitro studies have shown that mechanical stress can have an inhibitory effect on tumor growth. Due to the growth of gliomas in the confined cranium space, that effect may be significant enough to be incorporated into macroscopic growth models. The results in [9] indicated that mechanical stress did not affect proliferation rates but decreased the rate of apoptosis and that led to a compaction of cells, which was supported by an observable increase in cell density in case of stress inhibited tumors. It was hypothesized that the mechanical stress inhibits glioma growth by affecting its invasiveness, which in the reaction-diffusion growth model is represented by a Fickian diffusion. More experimental work would be needed to formulate an appropriate relation that would be physiologically consistent. It is known that gliomas invade white matter more aggressively than grey matter and anisotropic diffusion coefficients have been used previously in literature to account for those differences. The work presented in this paper used a spatially variant diffusivity that was only affected by mechanical stress caused by tumor growth. However heterogeneous diffusion coefficients for gray and white matter would be relatively straightforward to integrate into this model framework. The brain parenchyma was assumed to have a linear elastic response to stress but different material properties can be modeled by changing the constitutive relationships. This model also assumes no intervening therapy but that can be modeled by modifying the reaction diffusion equation as in [5]. In Model 3 a minimum threshold size of 1 cm was assumed before it starts exerting an inhibitory affect. A more appropriate value would have to be experimentally determined. While some parameter values were used from literature where they were available, all published models are unique and have their own set of assumptions. At times it was difficult to directly make use of those values and appropriate measures had to be determined by numerical experimentation. Since this was a preliminary investigation all the results presented in this paper are computational simulations and the next natural step would be use of the model to validate in vivo measures such as displacements caused by tumors in the brain parenchyma.

The computational simulations presented in this work show that stress could potentially have a significant effect on tumor growth. Two different implementations of a model where stress exerts an inhibitory effect on tumor growth were presented in this paper. In the Results sections part of the domain was clipped in presenting the results of Model 2 in Figure 3-5. This was done to ease the direct comparison of results from the two models because the stress acts on two slightly different domains. The displacements and radial stresses for the entire domain for Model 2 at one time point are shown in Figure 6.
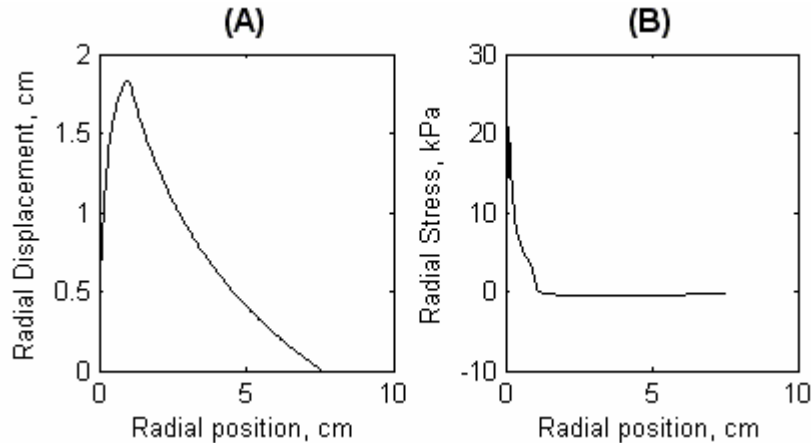
Figure 6: The (A) radial displacement and (B) radial stress for a time point in Model 2. As seen in panel (B), there is a strong tensile component of radial stress.

Part of the domain is in tension and while it is difficult to see due to scaling, the remainder is under compressive stresses (see panel B). The tensile effects are not consistent with physiological tumor growth. In that respect Model 3 might be a better choice. In the implementation of Model 3, the stress does not start to act or affect the growth until it reaches a certain threshold value. This is consistent with the finding in [9] that tumor spheroids grow in the mechanically resistant matrix until a growth-inhibitory threshold level of stress was attained. Also it is easier to directly use tumor front displacements to drive the mechanical model than empirically determining an indirect coupling factor for stress and

concentration gradient, i.e. λ in equation (5). The change in tumor radius as predicted by the three models is shown in Figure 7. Model 2 and Model 3 predict a slower tumor growth than Model 1. These curves qualitatively resemble the initial part of results shown in [9] with a few notable differences. Since this model is applicable to tumor on the order of 1 cm, and spheroids grow to the order of micrometers the scale for tumor size and growth time is very different. The plateau effects of growth at longer times are not seen in the results in Figure 7.
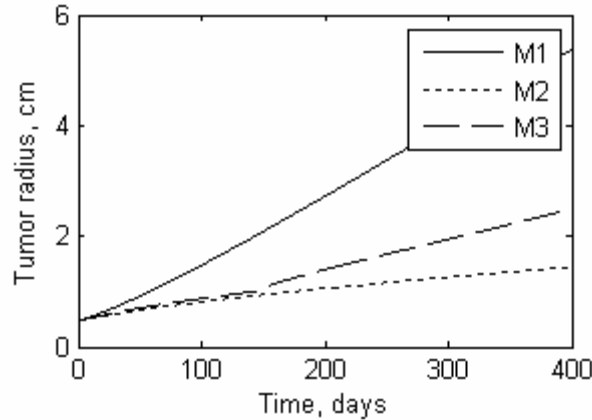
Figure 7: Change in tumor size as predicted by the three models over time.

That could be because of the aforementioned differences in medium of growth, temporal and spatial scales of tumor growth, or different tumor cell lines. The increase in tumor radius in 6 months as predicted by Models 1, 2 and 3 are 2 cm, 6 mm and 8mm respectively. As a comparison to a macroscopic glioma growth model an average tumor boundary displacement of 3 mm was reported in the same time period in [7]. The discrepancy could result from the choice of parameters. While all three models predict higher tumor boundary displacement than what is reported in [7], values predicted by Models 2 and 3 are much closer to the reported displacement.

5. CONCLUSIONS

There might be some benefit to integrating the insights gained from in vitro tumor growth models into macroscopic models for glioma growth. While the mathematical models for in vitro models afford the advantage of controlling and knowing more parameters and thus can be constructed with a greater degree of complexity for fine tuning such is not the case for macroscopic growth models. However it was demonstrated in this work that it might be worthwhile exploring some of the findings on that microscopic scale and applying them to macroscopic scale. The purpose of this study was a preliminary investigation into observing the inhibitory effects of stress and inferring general trends about the tumor growth. The simplicity provided by a single spatial dimension aids in a better understanding before a more complicated model can be pursued. Accurate macroscopic models of brain tumor growth could be used in many applications. For example, statistical atlases of brain function can be used in surgical guidance to prevent the surgical invasion of important functional areas of the brain (e.g. motor cortex). Often, these atlases are based on "normal" brains. Understanding the movement of these statistical distributions of functional areas in response to disease growth may be very important for improving a patient's quality of life post-surgical outcome. In addition, recent findings have indicated that significant swelling of the brain can occur from the very initiation of tumor resective therapy. To improve guidance systems, it may be advantageous to correlate the degree of swelling with an accurate biomechanical model of disease growth. In so doing, important information for preoperative planning could be derived as well as the potential for guidance correction during the earliest stages of surgery.

ACKNOWLEDGEMENTS

APPENDIX

The appendix lists the details of the implementation of some aspects of the model. The model was implemented in polar coordinates. Equation (1) expanded out in polar coordinates is shown below.

$$\frac{\partial c}{\partial t} = \left(\frac{\partial^2 c}{\partial r^2} + \frac{1}{r}\frac{\partial c}{\partial r} + \frac{1}{r^2}\frac{\partial^2 c}{\partial \theta^2} \right) + f(c) \qquad (6)$$

The equation (3) written for polar coordinates when f_{ext} is zero is shown below in matrix form.

$$\nabla \cdot \begin{bmatrix} \sigma_{rr} & \sigma_{r\theta} \\ \sigma_{\theta r} & \sigma_{\theta\theta} \end{bmatrix} = 0 \qquad (7)$$

For an axially symmetric problem, this equation reduces to the following [14].

$$\frac{\partial \sigma_{rr}}{\partial r} + \frac{1}{r}(\sigma_{rr} - \sigma_{\theta\theta}) = 0 \qquad (8)$$

The constitutive equations for the linear, elastic, homogenous, and isotropic material for plane strain in polar coordinates are shown below.

$$\varepsilon_{rr} = \frac{1}{E}[\sigma_{rr} - \upsilon\sigma_{\theta\theta}]$$

$$\varepsilon_{\theta\theta} = \frac{1}{E}[\upsilon\sigma_{rr} - \sigma_{\theta\theta}] \qquad (9)$$

$$\varepsilon_{r\theta} = \frac{1}{2G}\sigma_{r\theta} = \frac{1}{2G}\sigma_{\theta r} = \varepsilon_{\theta r}$$

In the equations above E is the Young's modulus of elasticity and υ is the Poisson's ratio. Since the terms $\sigma_{r\theta}$ and $\sigma_{\theta r}$ don't appear in equation (8), the remaining terms can be used to solve the equations for stresses in terms of strain.

$$\sigma_{rr} = \frac{E}{(1-\upsilon^2)}(\varepsilon_{rr} + \upsilon\varepsilon_{\theta\theta})$$

$$\sigma_{\theta\theta} = \frac{E}{(1-\upsilon^2)}(\upsilon\varepsilon_{rr} + \varepsilon_{\theta\theta}) \qquad (10)$$

The definitions of strain terms are shown below.

$$\varepsilon_{rr} = \frac{\partial u_r}{\partial r}$$

$$\varepsilon_{\theta\theta} = \frac{u_r}{r} + \frac{1}{r}\frac{\partial u_\theta}{\partial \theta} \qquad (11)$$

Thus strains were expressed in the form of displacements and the displacements were solved for in equation (8). The displacements obtained were then used to obtain the angular and radial stresses as expressed in equation (10).

REFERENCES

[1] Schwartzbaum, J. A., Fisher, J. L., Aldape, K. D. and Wrensch, M., "Epidemiology and molecular pathology of glioma," Nature Clinical Practice Neurology 2(9), 494-503 (2006).
[2] Greenwood, R., Barnes, M. P., McMillan, T. M. and Ward, C. D., [Neurological Rehabilitation], Psychology Press, 535-537 (1997).

[3] CBTRUS, "Statistical Report: Primary Brain Tumors in the United States, 1998-2002," http://www.cbtrus.org (2005).

[4] Swanson, K. R., Alvord, E. C., Jr. and Murray, J. D., "Virtual brain tumours (gliomas) enhance the reality of medical imaging and highlight inadequacies of current therapy," Br J Cancer 86(1), 14-18 (2002).

[5] Swanson, K. R., Bridge, C., Murray, J. D. and Alvord, E. C., Jr., "Virtual and real brain tumors: using mathematical modeling to quantify glioma growth and invasion," J Neurol Sci 216(1), 1-10 (2003).

[6] Jbabdi, S., Mandonnet, E., Duffau, H., Capelle, L., Swanson, K. R., Pelegrini-Issac, M., Guillevin, R. and Benali, H., "Simulation of anisotropic growth of low-grade gliomas using diffusion tensor imaging," Magn Reson Med 54(3), 616-624 (2005).

[7] Clatz, O., Sermesant, M., Bondiau, P. Y., Delingette, H., Warfield, S. K., Malandain, G. and Ayache, N., "Realistic simulation of the 3-D growth of brain tumors in MR images coupling diffusion with biomechanical deformation," IEEE Trans Med Imaging 24(10), 1334-1346 (2005).

[8] Stein, A. M., Demuth, T., Mobley, D., Berens, M. and Sander, L. M., "A mathematical model of glioblastoma tumor spheroid invasion in a three-dimensional in vitro experiment," Biophysical Journal 92(10), 356-365 (2006).

[9] Helmlinger, G., Netti, P. A., Lichtenbeld, H. C., Melder, R. J. and Jain, R. K., "Solid stress inhibits the growth of multicellular tumor spheroids," Nature Biotechnology 15(8), 778-783 (1997).

[10] Ambrosi, D. and Mollica, F., "The role of stress in the growth of a multicell spheroid," J. Math. Biol. 48(5), 477-499 (2004).

[11] Roose, T., Netti, P. A., Munn, L. L., Boucher, Y. and Jain, R. K., "Solid stress generated by spheroid growth estimated using a linear poroelasticity model," Microvascular Research 66(204-212 (2003).

[12] Cruywagen, G., Woodward, D., Tracqui, P., Bartoo, G., Murray, J. D. and Alvord, E. C., Jr., "The modeling of diffusive tumours," J. Biological Syst. 3(4), 937-945 (1995).

[13] Dumpuri, P., Thompson, R. C., Dawant, B. M., Cao, A. and Miga, M. I., "An atlas-based method to compensate for brain shift: preliminary results," Medical Image Analysis 11(2), 128-145 (2007).

[14] Boresi, A. P. and Chong, K. P., [Elasticity in Engineering Mechanics], John Wiley & Sons, New York, 438-451 (2000).